Many-body Anderson localization in one-dimensional systems

Dominique Delande, Krzysztof Sacha, Marcin Plodzień, Sanat K Avazbaev, Jakub Zakrzewski

PAPER • OPEN ACCESS

Many-body Anderson localization in one-dimensional systems

To cite this article: Dominique Delande *et al* 2013 *New J. Phys.* **15** 045021

View the article online for updates and enhancements.

Related content

Recent citations

Many-body Anderson localization in one-dimensional systems

Dominique Delande[1,5]**, Krzysztof Sacha**[2,3]**, Marcin Płodzień**[2]**, Sanat K Avazbaev**[1,4] **and Jakub Zakrzewski**[2,3]

[1] Laboratoire Kastler Brossel, UPMC-Paris6, ENS, CNRS; 4 Place Jussieu, F-75005 Paris, France
[2] Instytut Fizyki imienia Mariana Smoluchowskiego, Uniwersytet Jagielloński, ulica Reymonta 4, PL-30-059 Kraków, Poland
[3] Mark Kac Complex Systems Research Center, Uniwersytet Jagielloński, ulica Reymonta 4, PL-30-059 Kraków, Poland
[4] ARC Centre for Antimatter–Matter Studies, Curtin University of Technology, GPO Box U1987, Perth, Western Australia 6845, Australia
E-mail: Dominique.Delande@lkb.upmc.fr

Abstract. We show, using quasi-exact numerical simulations, that Anderson localization in a disordered one-dimensional potential survives in the presence of attractive interaction between particles. The localization length of the particles' center of mass—computed analytically for weak disorder—is in good agreement with the quasi-exact numerical observations using the time evolving block decimation algorithm. Our approach allows for simulation of the entire experiment including the final measurement of all atom positions.

[5] Author to whom any correspondence should be addressed.

IOP Institute of Physics **Φ** DEUTSCHE PHYSIKALISCHE GESELLSCHAFT

Contents

1. Introduction

Anderson localization (AL) has been widely investigated in the last 50 years [1, 2]. The possibility of directly observing localization of the wavefunction in cold atomic gases has led to a recent revival of interest in localization properties in general, and in AL in particular. AL is characterized by the inhibition of transport in a quantum system, whose classical counterpart behaves diffusively. It is accompanied by an exponential localization of eigenstates in the configuration space, $|\psi(r)|^2 \propto \exp(-|r|/L)$, where L is the localization length. AL is due to the interference between various multiple scattering paths which favors the return of the particle to its initial position and thus decreases the probability of it traveling a long distance. As the geometry of these paths depends on the system dimension, so AL features depend on the dimension too. For one-dimensional (1D) systems, AL is a generic single-particle behavior even for very small disorder when the particle 'flies' above the potential fluctuations.

A fundamental question is to understand how interaction between particles affects AL. Presently, there is no consensus on the possible existence and properties of many-body localization. Some results suggest that AL survives for few-body systems, although with a modified localization length [3]; studies of cold bosonic systems in the mean-field regime show that AL is destroyed and replaced by a sub-diffusive behavior [4, 5], but the validity of the mean-field approximation at long times is questionable. There are even predictions that AL survives at finite temperature in the thermodynamic limit, in the presence of interactions [6]. In this paper, we show, using a specific example, that 1D AL survives in the presence of attractive interactions and is even a rather robust phenomenon. The novelty of our approach is that it uses a quasi-exact numerical scheme to solve the full many-body problem in the presence of disorder. Here, quasi-exact means that all numerical errors can be controlled and reduced below an arbitrary value, just at the cost of increased computational resources. The big advantage of this approach is not to rely on neglecting *a priori* any physical process.

Atomic matter waves have several advantages that made possible an unambiguous demonstration of single-particle AL in 1D [7, 8]: atom–atom interaction can be reduced by either diluting the atomic gas or using Feshbach resonances, ensuring a very long coherence time of the atomic matter wave; the spatial and temporal orders of magnitude are very convenient, allowing a direct spatio-temporal visualization of the dynamics; all microscopic ingredients are well controlled; and a disordered potential can be created by using the effective potential induced by a far detuned optical speckle.

2. The model and its solution

We consider N identical bosonic atoms in a 1D system, in the regime of attractive two-body interactions. We assume the dilute regime where the atom–atom average distance is larger than the scattering length and take the low-energy limit where the interaction can be modeled by a (negative) Dirac-delta potential. The many-body Hamiltonian can be written, using the standard second quantization formalism (assuming unit mass for the particles and taking $\hbar = 1$):

$$\hat{H} = \int dz \; \hat{\psi}^{\dagger}(z) \left[-\frac{1}{2}\frac{\partial^2}{\partial z^2} + V(z) \right] \hat{\psi}(z)$$
$$+ \frac{g}{2} \int dz \; \hat{\psi}^{\dagger}(z) \, \hat{\psi}^{\dagger}(z) \, \hat{\psi}(z) \, \hat{\psi}(z), \tag{1}$$

where $g < 0$ is the strength of the atom–atom interaction and $V(z)$ is an external potential.

For large N, in the absence of an external potential, the ground state of this system is described—within the mean field approach—as a bright soliton, a composite particle with two external degrees of freedom: an irrelevant phase θ, and a classical parameter: the position q of the center of mass. The particle density—normalized to the number N of particles—is given by $|\phi_0(z-q)|^2$ where

$$\phi_0(z) = \sqrt{\frac{N}{2\xi}} \frac{e^{-i\theta}}{\cosh z/\xi}. \tag{2}$$

$\xi = -\frac{2}{Ng}$ is the characteristic size of the soliton. The associated chemical potential is $\mu = -N^2 g^2/8$.

This mean-field approach does not describe properly the many-body ground state of the system. Indeed, in the absence of an external potential, the many-body ground state is known exactly, thanks to the Bethe ansatz [9] which predicts e.g. uniform atomic density. The source of discrepancy lies in a classical treatment of the center of mass q of the system. In a proper description, q must be thought of as the quantum position operator of the soliton, the composite particle formed by the N particles. In the presence of an external potential, it is possible to construct an effective one-body (EOB) Hamiltonian describing the q dynamics quantum mechanically [10–13]. Assuming a fixed soliton shape, the EOB Hamiltonian is

$$H_q = \frac{p_q^2}{2N} + \int dz \, |\phi_0(z-q)|^2 \, V(z), \tag{3}$$

where p_q is the momentum conjugate to q [10–13]. It describes a composite particle with mass N evolving in a potential that is the convolution of the bare potential with the soliton envelope. The key point of the EOB approach is that the internal degrees of freedom of the soliton are hidden in the reduction of the many-body wavefunction to a single one-body wavefunction $\varphi(q, t)$ describing the evolution of the soliton center of mass. This is possible because the internal degrees of freedom of the bright soliton are gapped, with an energy gap equal to $-\mu = N^2 g^2/8$, so that a weak external perturbation cannot populate internal excited states of the bright soliton, in contrast with the dark soliton case [14].

Because the EOB Hamiltonian (3) describes a 1D system exposed to a disordered potential, it displays AL. Within the EOB approximation, the soliton center of mass is localized with a localization length depending on the energy. As an example, we will use—as in real experiments [7]—the disorder created by a light speckle shone on a cold atomic gas.

The localization length of the EOB model has been calculated (in the weak disorder limit) in [11–13]:

$$\frac{1}{L_N(k)} = \frac{N^4 \xi^2 \pi^3 \sigma_0 V_0^2 (1 - k\sigma_0)}{\sinh^2 \pi k \xi} \Theta(1 - k\sigma_0), \tag{4}$$

where k is the wavevector of the soliton, V_0 the rms amplitude of the disordered potential, σ_0 its correlation length of the speckle and Θ the Heaviside function.

What is the validity of the EOB theory at long time? The answer is far from obvious. Any many-body effect not taken into account within the EOB could break the reduction of the problem into an EOB wavefunction evolving under the effective Hamiltonian (3). In particular, it could easily spoil the phase coherence of the EOB wavefunction and consequently AL. It is the goal of this paper to perform a quasi-exact many-body numerical test of the EOB approach. In order to be as close as possible to a realistic experiment [7], we follow the temporal evolution of an initially localized many-body wavepacket. In a first step, we compute the ground state of N interacting particles in the presence of a harmonic trap, but without disorder: this produces a bright soliton localized near the trap center. In a second step, the harmonic trap is abruptly switched off and the disordered speckle potential abruptly switched on, leaving the many-body system to expand in the presence of disorder, and eventually localize thanks to many-body AL.

In the presence of an external potential, the many-body problem cannot be solved exactly. One must rely on quasi-exact numerical approaches. A convenient way is to discretize the continuous Hamiltonian, equation (1), over a discrete lattice [15, 16]. The discretization of space to a chain of sites located at equally spaced positions $z_l = l\delta$ together with a three-point discretization of the Laplace operator allows us to write the Hamiltonian in a tight-binding Bose–Hubbard form [15]

$$H = \sum_l \left[-J(a_l^\dagger a_{l+1} + \text{h.c.}) + \frac{U}{2} a_l^\dagger a_l^\dagger a_l a_l + V_l\, a_l^\dagger a_l \right] \tag{5}$$

with $J = \frac{1}{2\delta^2}$, $U = \frac{g}{\delta}$ and $V_l = V(z_l)$ (an additional trivial constant term $1/\delta^2$ has been dropped).

For numerical purposes the infinite space is restricted to the $[-K\delta, K\delta]$ interval leading to a 1D chain of $M = 2K + 1$ discrete sites. N identical bosons are distributed on these M sites. A basis of the total Hilbert space can be built using the direct product of Fock states on each site $|i_1, i_2, \ldots, i_M\rangle$ with the constraint that the sum of occupation numbers $\sum_{l=1,\ldots,M} i_l$ is equal to N. The size of this basis increases exponentially with the system size, making its use unpractical for large many-body problems. Instead, we use a variational set of matrix product states (MPSs). An MPS is a state which can be written as

$$|\psi\rangle = \sum_{\alpha_1,\ldots,\alpha_M;\ i_1,\ldots,i_M} \Gamma^{[1],i_1}_{1\alpha_1} \lambda^{[1]}_{\alpha_1} \Gamma^{[2],i_2}_{\alpha_1\alpha_2}, \ldots, \Gamma^{[M],i_M}_{\alpha_{n-1}1} |i_1, \ldots, i_M\rangle, \tag{6}$$

where $\Gamma^{[l],i_l}$ ($\lambda^{[l]}$) are site (bond)-dependent matrices (vectors). To describe exactly a generic state in terms of MPSs, a large number (exponentially increasing with M) of α_l values is needed. However, typical low-energy states are only slightly entangled so that $\lambda^{[l]}_{\alpha_l=1,2\ldots}$ are rapidly decaying numbers, which allows for introduction of a cutoff χ in the sum over Greek indices above, resulting in tractable numerical computations [17]. For a ground state protected by a gap, the area theorem [18] ensures that an efficient MPS representation exists. In the physical situation discussed by us, the area law has no direct applicability.

The $i_1, \ldots, i_M$ indices are, in principle, restricted to the $[0, N]$ interval. In practice, since it is highly unlikely that all the bosons occupy a single site of the system, we lower the cutoff in

the sums assuming some $N_{max} < N$. While the maximum average occupation number (at sites near the center of mass of the soliton) is $N\delta/2\xi = 2.5$, we found surprisingly that a relatively high $N_{max} = 14$ is needed for convergent results, while the χ value may be kept relatively low.

The ground state as well as the dynamics may be quasi-exactly studied using the time evolving block decimation (TEBD) algorithm [17, 19], essentially equivalent to the time-dependent density matrix renormalization group approach [20, 21]. The TEBD algorithm describes how the $\Gamma^{[l]}$ and $\lambda^{[l]}$ evolve in time under the influence of a Hamiltonian containing simple terms local on each site as well as hopping terms of the type $a_l a_{l+1}^\dagger$ which transfer one particle from site l to site $l+1$. A maximum of $N = 25$ particles could be included in our calculations; similar results are obtained for ten particles.

We use the soliton size ξ as the unit of length; consequently the time unit is ξ^2. We use the EOB as a guide to choose the parameters of the many-body numerical experiment. For example, the trap must be shallow enough not to distort the soliton shape (2), but still strong enough to confine its center of mass q over a distance only slightly larger than its size. We chose $\Delta q = \sqrt{\frac{8}{5}}\xi$; the frequency, ω, of the trapping harmonic potential $\omega^2 z^2/2$ is thus such that $N\omega = 5/8\xi^2$, i.e. $\omega = 0.025/\xi^2$. In order for the localization length to be reasonably short, we choose the strength of the external potential comparable to the initial average energy of the soliton $\omega/4$, that is $V_0 = 2.5 \times 10^{-4}$. We also choose the correlation length of the speckle potential $\sigma_0 = 0.4\xi$ to be significantly shorter than the soliton size, so that the EOB potential in equation (3) is free of the peculiarities of the speckle potential [26].

Several sources of errors exist in the TEBD algorithm and must be controlled. The first one is due to the spatial discretization. Getting accurate results requires the discretization unit, δ, to be much smaller than both the soliton size ξ and the de Broglie wavelength $2\pi/k$, where k is the typical wavevector contained in the initial wavepacket for the center of mass in the EOB description. We use $\delta = \xi/5$; a twice smaller step produces slightly different quantitative results, but the difference is practically invisible on the scale of the figures shown in our work. In order to avoid reflections from the boundaries, the number of lattice points must be sufficiently large; 1921 points are used, but only the central 1201 ones are shown in the plots. A second source of error is the temporal discretization of the evolution operator. We use the standard Trotter expansion [17], whose error can be controlled by varying the time step ($\delta t = 0.008\xi^2$ is used). A third source of error is the truncation of the MPS at each step. This error is monitored through the so-called 'discarded weight', that is the weight of the components which have to be discarded from the time evolved many-body state to keep it in MPS form with a fixed parameter χ—the number of bonds between sites. This can be a serious problem when the entropy of entanglement grows as a function of time. It may even prevent calculation to be run beyond some rather short time, especially when the system is significantly excited above the ground state [22].

The entropy of entanglement is defined as the supremium over all possible bipartitions of the system. Explicitly, we compute

$$S = \sup_l S_l = \sup_l \left[-\sum_\alpha (\lambda_\alpha^{[l]})^2 \ln(\lambda_\alpha^{[l]})^2 \right] \tag{7}$$

with l running over all bonds. Typically, the maximum is reached for a link close to the center of the system but it can depend on the disorder and fluctuate in time. Quite surprisingly, we have not observed any significant growth of the entropy of entanglement when AL sets in, see
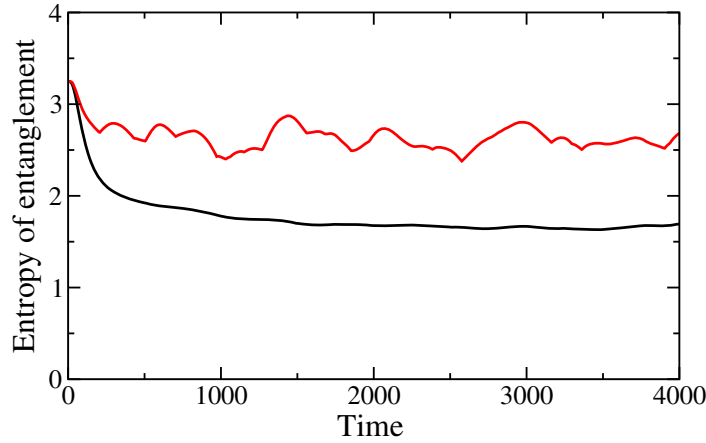
Figure 1. Time evolution of the entropy of entanglement, equation (7), for an initially localized bright soliton expanding in a disordered speckle potential, obtained using the many-body TEBD algorithm. No significant growth of the entropy is observed. The red curve is the largest entropy among 96 different realizations of disorder while the black curve corresponds to the average over these realizations. Parameters are given in the text.
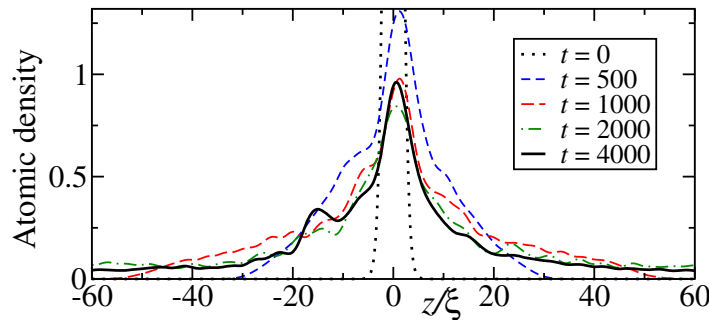

Figure 2. Spatial atomic density of an initially localized bright soliton, under the influence of a disordered speckle potential, using the quasi-exact many-body TEBD algorithm, at various times. After an initial expansion, the atomic density freezes at long time, a signature of many-body AL. Parameters are given in the text. The results presented are averaged over 96 realizations of the disorder.

figure 1, a result quite opposite to that observed in [23]. This may be attributed to the fact that the energy of our many-body state is quite small (see the discussion above). The converged calculations reported here use $N_{max} = 14$, $\chi = 30$ yielding the internal Hilbert space dimension per site as 450. The results have been compared with those with lower N_{max} as well as those for $\chi = 40$ (for shorter times) to check that the results presented are fully converged. All in all, we were able to run the fully controlled calculation up to time $t = 4000$.

Figure 2 shows the particle density in configuration space obtained at increasing times averaged over 96 realizations of the disorder. In the absence of disordered potential, the initial wavepacket is expected to spread ballistically. The EOB physics gives the characteristic time
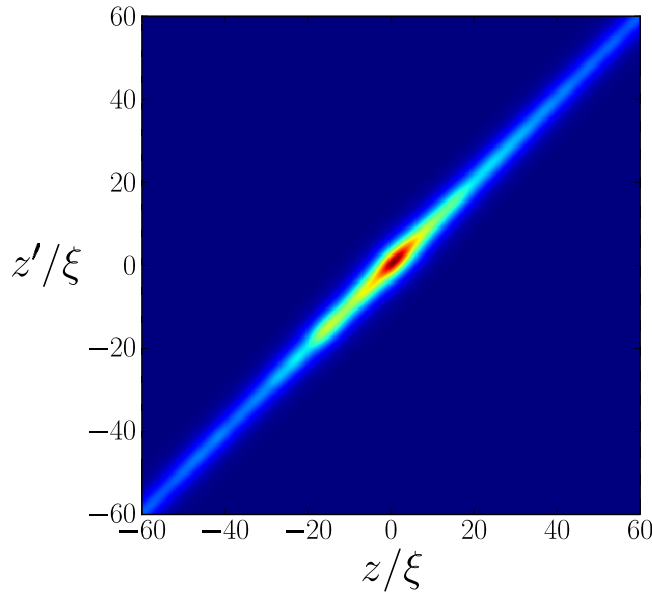
Figure 3. One-body density matrix of the many-body state at $t = 4000$ (see figure 2) in configuration space. It is strongly concentrated along the diagonal $z = z'$ with a transverse width of the order of the soliton size ξ. This is a direct proof that the many-body system can be described by a compact composite particle, a bright soliton, whose center of mass is widely spread.

for this spreading, $t = 1/\omega = 40$, much shorter than the time scale in the figure. At $t = 500$ and 1000, one clearly sees that the central part of the wavepacket is already more or less localized while the ballistic front for $|z|/\xi > 20$ ($|z|/\xi > 40$ for $t = 1000$) has not yet been scattered and keeps a Gaussian shape similarly as in the EOB description. This corresponds to the wavepacket components with the highest energy and consequently the longest localization length. AL has already been set up at $t = 2000$ and does no longer evolve further, compare with $t = 4000$. Therefore, figure 2 provides evidence for many-body AL taking place in a quasi-exact full many-body numerical simulation. At the final time (100 times the characteristic spreading time), we do not observe any indication that AL could be destroyed.

The description of the final state as an MPS makes it possible to easily compute more complicated quantities, such as correlation functions. The simplest is the one-body density matrix $\langle \psi^\dagger(z)\psi(z')\rangle$, shown in figure 3. It clearly displays extremely strong correlations between positions z and z', reinforcing the observation that AL probably survives far beyond $t = 4000$. The interpretation is simple in terms of bright solitons: all atoms are grouped in a soliton of size ξ, but the center of mass of the soliton itself is widely spread. This has an important consequence: the largest eigenvalue of the one-body density matrix—a value often used as a quantitative criterion for Bose–Einstein condensation [27]—is on average 0.14, much smaller than unity; in contrast, the value at $t = 0$ is 0.84. Thus, while the initial state can be considered as a true condensate, the temporal dynamics destroys condensation; any description of our many-body system using the mean field theory via the Gross–Pitaevskii equation (which by construction describes a 100% condensate) *must* fail. In other words, our many-body AL is necessarily beyond the mean field description.
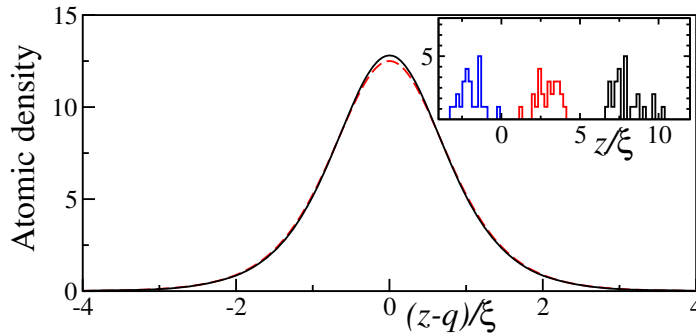
Figure 4. Atomic density measured with respect to the center of mass of the N particles, at time $t = 4000$, after AL has set in. A large number of individual 'measurements' of the particle positions—three examples are shown in the inset—are performed for various disorder realizations, and the resulting average is displayed in the main panel. The agreement between the full many-body calculation (solid line) and the prediction of equation (2) for the soliton shape (dashed line) is excellent.

3. Simulation of a measurement

Being able to write the many-body state as an MPS has considerable further advantages, especially if it is—like in our calculations—in the so-called canonical form [21]. For example, expectation values of local operators such as $a_l^\dagger a_l$ or $a_l^\dagger a_{l+1}$ involve only simple contractions on the local $\Gamma^{[l]}$ tensors and $\lambda^{[l]}$ vectors. It makes it also possible to mimic the measurement process of particle positions as follows. The reduced density matrix $\rho^{[l]}$ on site l is easily constructed by contracting the $\Gamma^{[l]}$ tensor with the neighboring $\lambda^{[l-1]}$ and $\lambda^{[l]}$ vectors:

$$\rho_{j,i}^{[l]} = \sum_{\alpha_{l-1},\alpha_l} [\lambda_{\alpha_{l-1}}^{[l-1]}]^2 \, \Gamma_{\alpha_{l-1}\alpha_l}^{[l],i} \, [\Gamma_{\alpha_{l-1}\alpha_l}^{[l],j}]^* \, [\lambda_{\alpha_l}^{[l]}]^2. \tag{8}$$

We then randomly choose the number of particles 'measured' on site l following the statistical populations, diagonal elements of the on-site reduced density matrix. Once a given occupation number i is chosen, we project the MPS state onto the subspace with $i_l = i$ and normalize it. This involves only simple contractions on the local Γ tensors and λ vectors, producing another MPS. The process can be iterated on all sites, and is particularly simple if sites are scanned consecutively starting from one edge and propagating toward the other edge. It is simple to prove that the probability distribution of the measurements is independent of the order used for scanning the various sites.

An individual 'measurement' produces a single set of occupation numbers $(i_1, i_2, \ldots, i_M)$ (whose sum is of course N) whose probability is exactly $|\langle i_1, i_2, \ldots, i_M | \psi \rangle|^2$. By performing a series of 'measurements', we can sample interesting physical quantities, such as the position of the soliton center of mass, $\langle q \rangle = \sum_l l \delta i_l / N$, and the particle density with respect to this center of mass. Note that these quantities are hard to measure by other means as they involve correlation functions of high order (typically up to N) [24, 25].

Examples of our procedure are given in the inset of figure 4. In this way, we extract both the position of the center of mass of the soliton and the atomic density relative to the center of mass. The latter quantity is shown in figure 4 for time $t = 4000$ in comparison with the analytic
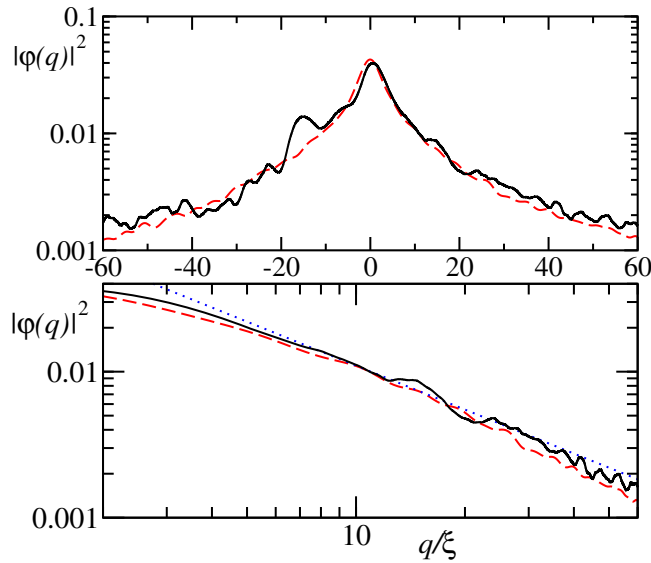
Figure 5. Probability density for the center of mass of the soliton at time $t = 4000$, numerically computed using the many-body quasi-exact dynamics (solid line, averaged over 96 disorder realizations) and the EOB theory (dashed line, averaged over 10 000 realizations). The good agreement shows that the many-body problem actually displays AL, as predicted by a simple theory for a composite particle. The dotted line in the lower panel (double logarithmic plot) is the $1/|q|$ approximate prediction of the EOB theory [11].

prediction, equation (2). The agreement is excellent, showing that the internal structure of the soliton is fully preserved for a long time, even after AL has set in. The small difference is a $1/N$ finite size effect.

4. Comparison with the effective one-body approach

The EOB theory is able to quantitatively predict the long time limit for the spatial density probability of the soliton center of mass, see the detailed derivation and calculations in [11]. Initially, the center of mass is in the ground state of the harmonic trap (a Gaussian wavepacket) that, after the trap is switched off, expands over a range of energies, each energy component being characterized by its own localization length. Each component displays approximate exponential localization in the long time limit (in a 1D system, Anderson localized eigenstates do not strictly decay exponentially, see e.g. [28, 29]). Their superposition displays approximate algebraic localization at long distance, as discussed in [11].

In figure 5, we show the comparison between the full many-body calculation and the EOB corresponding numerical simulation with Hamiltonian (3). Note that the many-body result is here plotted for the center-of-mass position, which can slightly differ from the atomic density; the latter, in the EOB approach, is the convolution of the former by the soliton shape. At the scale of the figure, the soliton is extremely narrow so that the result of the convolution is almost equal to the center-of-mass density, compare with figure 2. The agreement between the many-body and the EOB calculations is clearly excellent. In figure 5, we also show the $1/|q|$ leading

behavior predicted by the EOB theory, equation (13) of [11]. It predicts the observed behavior quite well but does not aim at being quantitative, because of the existence of a sub-leading logarithmic term. Namely, at very large distance, the exponential term $\exp[-\beta \ln^2(\gamma |q|)]$, where γ and β are constants, present in equation (13) of [11] becomes important, leading to a faster decrease of the distribution and eventually to a finite rms displacement $\langle q^2 \rangle$ of the soliton. Note also that the formula, equation (13) of [11], assumes a weak disorder (Born approximation), an assumption not fully satisfied here.

Finally, we compare the localization length of the center of mass of attractively interacting particles with the localization length of a single particle in the same disordered potential. A meaningful comparison must be performed for the same total energy per particle, or equivalently for the same wavevector per particle; this thus corresponds to a wavevector N times larger for the soliton, composed of N individual particles. Within the EOB approach, the ratio is, for $k\sigma_0 < 1$ and weak disorder,

$$\frac{L_1(k/N)}{L_N(k)} = N^2 \left[\frac{\pi k \xi}{\sinh \pi k \xi} \right]^2 \frac{1 - k\sigma_0}{1 - k\sigma_0/N}. \tag{9}$$

The physical interpretation is simple and interesting. The N^2 factor strongly favors localization of the soliton and reflects the collective behavior of the N attractive bosons when placed in the disordered potential. The second factor—and to a lesser extent, the third one—is smaller than unity and favors delocalization of the soliton. It reflects the fact that the center of mass of the soliton does not feel the raw potential, but rather its convolution with the soliton shape, see equation (3); being smoother, the convoluted disordered potential scatters less efficiently than the raw one, leading to an increase of the localization length. It is ultimately due to the dispersion of the atom positions around the center of mass of the soliton. Whether the localization or the delocalization effect wins depends on the parameter values. For the parameters used here, if $k\xi > 1.8$, the localization length of the soliton is longer than the single atom localization length, shorter otherwise. Thus, no general statement on whether attractive interactions favor AL or not can be made.

5. Summary

To summarize, we have shown the existence of many-body AL for attractive bosons in the presence of a disordered potential. The claim is based on quasi-exact many-body numerical simulations using the TEBD algorithm, which incorporate all complicated phenomena that could spoil the internal phase coherence of the many-body composite object, a bright soliton, displaying AL. Moreover, we obtain excellent agreement between the many-body calculation and a one-body effective theory, which goes beyond standard mean field theories such as the Gross–Pitaevskii equation. Our quasi-exact many-body approach allows for simulation of the entire experiment starting from the initial state in a harmonic trap till the destructive measurement of all atom positions.

Acknowledgments

IOP Institute of Physics ⬧ DEUTSCHE PHYSIKALISCHE GESELLSCHAFT

References

[1] Anderson P W 1958 *Phys. Rev.* **109** 1492
[2] Lagendijk A, van Tiggelen B A and Wiersma D S 2009 *Phys. Today* **62** 24
[3] Shepelyansky D L 1994 *Phys. Rev. Lett.* **73** 2607
[4] Pikovsky A S and Shepelyansky D S 2008 *Phys. Rev. Lett.* **100** 094101
[5] Ivanchenko M V, Laptyeva T V and Flach S 2011 *Phys. Rev. Lett.* **107** 240602
[6] Aleiner I L, Altshuler B L and Shlyapnikov G 2010 *Nature Phys.* **6** 900
[7] Billy J *et al* 2008 *Nature* **453** 891
[8] Roati G *et al* 2008 *Nature* **453** 895
[9] McGuire J B 1964 *J. Math. Phys.* **5** 622
[10] Weiss C and Castin Y 2009 *Phys. Rev. Lett.* **102** 010403
[11] Sacha K, Müller C A, Delande D and Zakrzewski J 2009 *Phys. Rev. Lett.* **103** 210402
[12] Sacha K, Delande D and Zakrzewski J 2009 *Acta Phys. Pol.* A **116** 772
[13] Müller C A 2011 *Appl. Phys.* B **102** 459
[14] Mochol M, Płodzień M and Sacha K 2012 *Phys. Rev.* A **85** 023627
[15] Schmidt B and Fleischhauer M 2007 *Phys. Rev.* A **75** 021601
[16] Glick J A and Carr L D 2011 arXiv:1105.5164
[17] Vidal G 2003 *Phys. Rev. Lett.* **91** 147902
[18] Eisert J, Cramer M and Plenio M B 2010 *Rev. Mod. Phys.* **82** 277
[19] Vidal G 2004 *Phys. Rev. Lett.* **93** 040502
[20] White S R and Feiguin A E 2004 *Phys. Rev. Lett.* **93** 076401
[21] Schollwöck U 2011 *Ann. Phys.* **326** 96
[22] Daley A J, Kollath C, Schollwöck U and Vida L G 2004 *J. Stat. Mech.* **2004** P04005
[23] Bardarson J H, Pollmann F and Moore J E 2012 *Phys. Rev. Lett.* **109** 017202
[24] Dziarmaga J, Deuar P and Sacha K 2010 *Phys. Rev. Lett.* **105** 018903
[25] Mishmash R V and Carr L D 2010 *Phys. Rev. Lett.* **105** 018904
[26] Lugan P *et al* 2009 *Phys. Rev.* A **80** 023605
[27] Pethick C J and Smith H 2001 *Bose Einstein Condensation in Dilute Gases* (Cambridge: Cambridge University Press)
[28] Gogolin A A 1988 *Phys. Rep.* **166** 269
[29] Müller C A and Delande D 2010 Disorder and interference: localization phenomena *Ultracold Gases and Quantum Information* (*Les Houches Summer School Session XCI*) ed C Miniatura *et al* (Oxford: Oxford University Press)